Materials Science & Engineering A 702 (2017) 265–271

Contents lists available at ScienceDirect

Materials Science & Engineering A

journal homepage: www.elsevier.com/locate/msea

Strain localization and crack formation effects on stress-strain response of ductile iron

Keivan A. Kasvayee[a,*], Ehsan Ghassemali[a], Kent Salomonsson[a], S. Sujakhu[b], S. Castagne[b], Anders E.W. Jarfors[a]

[a] School of Engineering, Jönköping University, Box 1026, 551 11 Jönköping, Sweden
[b] School of Mechanical and Aerospace Engineering, Nanyang Technological University, Singapore 639798, Singapore

ARTICLE INFO

Keywords:
In-situ tensile test
Digital image correlation
Micro-crack
Graphite-matrix decohesion
Cracking

ABSTRACT

The strain localization and crack formation in ferritic-pearlitic ductile iron under tension was investigated by in-situ tensile tests. In-situ tensile tests under optical microscope were performed and the onset of the early ferrite-graphite decohesions and micro-cracks inside the matrix were studied. The results revealed that early ferrite-graphite decohesion and micro-cracks inside the ferrite were formed at the stress range of 280–330 MPa, where a kink occurred in the stress-strain response, suggesting the dissipation of energy in both plastic deformation and crack initiation. Some micro-cracks initiated and propagated inside the ferrite but were arrested within the ferrite zone before propagating in the pearlite. Digital Image Correlation (DIC) was used to measure local strains in the deformed micrographs obtained from the in-situ tensile test. Higher strain localization in the microstructure was measured for the areas in which the early ferrite-graphite decohesions occurred or the micro-cracks initiated.

1. Introduction

The material microstructure governs the material properties and the component performance. Inhomogeneous microstructure can give rise to local variations in the microstructural properties, e.g. the elastic-plastic behavior [1], volume fraction and phase arrangement [2,3]. This can result in local stress concentration causing crack initiation. Similarly, microstructure defects such as inclusions and pores can cause local stress concentration resulting in crack initiation during loading through particle cracking or particle-matrix decohesion. In-situ tensile test can be used to characterize the crack initiation processes associated to the multi-phase materials [4,5]. Combining in-situ tensile testing with digital image correlation (DIC) [6,7] allows quantitative studies of strain distribution in the microstructure [8] and in the vicinity of cracks [9–11].

Ductile iron is a multiphase material with ferrite, pearlite and graphite as constituents [12]. The properties between the constituents are very different resulting in a heterogeneous deformation at the micro-scale, in particular around graphite particles [13–15]. The arrangement of the phases will result in a significant scatter in the local response of the material to the loading, especially during deformation, crack initiation and propagation.

Graphite particles (both nodules and degenerated nodules) in ductile iron cause stress and strain concentration on loading [16]. If the local strain exceeds a critical level, a micro-crack may form [11]. The differences in elastic and plastic properties between graphite and matrix can raise the stress in the interface of the graphite particles and eventually can cause interfacial decohesion and/or crack initiation [17]. Stokes et al. [18] considered the graphite-matrix decohesion as the critical micromechanisms for initiation and growth of micro-cracks. Decohesion was mostly reported when a perfectly round nodule was surrounded by a ferrite phase [5,19]. In addition, the irregular surface and sharp corners of graphite can promote the interfacial crack initiation [20].

Several studies have been focused on simulating the strain distribution and crack formation for multiphase materials at the microstructural level [21–23]. Different modeling techniques have been used to model crack initiation and propagation. The predominant method used over the past decade is the extended Finite Element Method (XFEM) due to its advantage of crack path independence [24,25]. The most common way to validate the simulation predication is the capability to reproduce the macroscopic experimental stress-strain [26,27]. However, multiscale modeling requires more deformation details at the microstructural scale. One potential route to obtain this information is through DIC, enabling a quantitative comparison of the strain distribution at the microstructural scale with validation of events such as

* Corresponding author.
E-mail address: Keivan.Amiri-Kasvayee@ju.se (K.A. Kasvayee).

http://dx.doi.org/10.1016/j.msea.2017.07.018
Received 13 April 2017; Received in revised form 10 July 2017; Accepted 11 July 2017
Available online 12 July 2017
0921-5093/ © 2017 Elsevier B.V. All rights reserved.

decohesion and micro-cracking.

The aim of this study is to investigate the effect of matrix-graphite decohesion and micro-crack initiation on the localized strain and stress-strain response of the ferritic-pearlitic ductile iron. In-situ tensile tests under optical microscope were performed to record the deformation micrographs up to fracture of the samples. The stress and strain at the onset of the early plastic deformation, ferrite-graphite decohesion and micro-cracks inside the matrix were investigated in relation to the changes in the slope of the tensile curve. Applying DIC to the deformed micrographs, localized strains at the onset of the micro-cracks were measured. This study is an extension of a previous work in which the strain distribution was quantified in the deformed microstructure excluding crack formation [28]. The scope of this work is to study the microstructural deformation including crack formation.

2. Experimental

2.1. Material

Ductile iron grade GJS-500-7 was sand cast as plates in a variety of the thicknesses. In the current study, the 30 mm thick plate was used as it showed a suitable variation in microstructure to study crack formation and decohesion. Table 1 represents the chemical composition of the material. The material had a eutectic composition. The carbon equivalent was calculated based on Eq. (1).

$$C_{eq} = \%C + 0.25(\%Si) + 0.33(\%P) + 0.41(\%S) \quad (1)$$

Where $\%C$, $\%Si$, $\%P$, and $\%S$ are the carbon, silicon, phosphorous and sulfur content (wt%), respectively.

The microstructure consisted of nodular and irregular-shaped graphite particles surrounded by a ferritic-pearlitic matrix, see Fig. 1. The amount of the constituents was 29 ± 1% ferrite, 63 ± 1% pearlite and 7 ± 1% graphite. The nodularity (by area) was 71 ± 3%, based on ASTM E 2567 [29].

2.2. In-situ tensile test

In-situ tensile test was performed at room temperature using a miniature tensile stage (TSL Solution KK., maximum load cell capacity (1200 N) mounted on an inverted optical microscope (Olympus GX81). Five samples identified as sample 1–5 were machined from the cast plate and were tested. Fig. 2 shows a sample schematic with dimensions in mm. The tests were performed with a crosshead speed of 3.3 μm/s. To allow for microscopy, the surface of the samples was grinded and polished. The thickness of the samples was machined to 1 ± 0.1 mm to enable tensile testing to be undertaken in the range of the maximum load capacity. The 1 mm thick samples showed similar tensile properties compared to a 0.7 mm thick sample. In addition, these samples fulfilled the mechanical properties according to standard (see Table 2), hence, no significant size effect was observed for the 1 mm thick samples.

The direct data output from the miniature tensile stage was overall load and crosshead displacement, which were used to measure the overall stress and strain of the samples. The values were recorded every second during in-situ tensile test. To compensate the tensile stage stiffness, a correctional equation was developed to reduce errors of displacement data and obtain reliable results. The equation was calculated by tensile testing a stiff sample, in which an extensometer was mounted on the tensile sample to measure the displacement during the tensile test. Then, the differences between the displacement data obtained using the machine and the extensometer were compared at various force amplitudes to determine the correction equation. Table 2 presents the average of tensile properties measured by the miniature tensile stage for the 5 samples.

The optical micrographs were recorded during deformation by a microscope camera (Olympus UC30), using one autofocusing function after each record, resulting in a picture every 6 s. Autofocusing compensated the out of plane deformation of the samples, due to the Poisson effect. Images were recorded in grey scale with the size of 2080 × 1544 pixels, giving a pixel size and imaging area of 0.54 μm/pixel and 0.96 mm^2, respectively.

After fracture of the in-situ tensile samples, scanning electron microscope (SEM), model JSM-700IF, in a secondary electron mode was used to examine the micro-cracks that were developed on the surface of the samples.

In this work, a micro-crack was defined as a microstructurally short crack, which was developed at the interface of the graphite and the

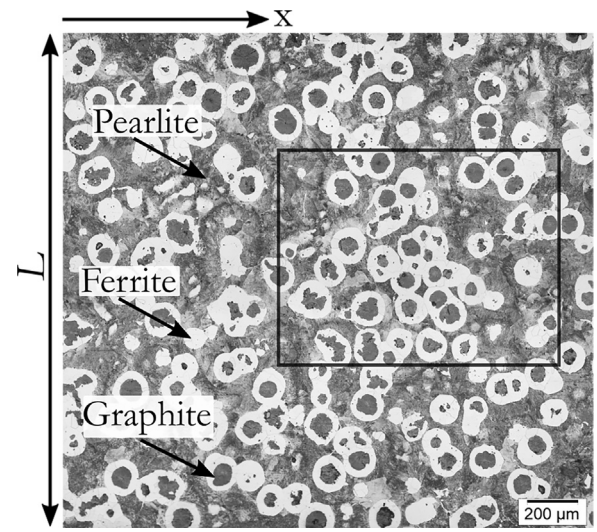

Fig. 1. Microstructure of the cast material obtained from the surface of the in-situ tensile sample 5; graphite particles (dark grey), ferrite (white) and pearlite (lamellar light grey). Etched in 5% Nital. *L* denotes the width of the in-situ tensile sample (2 mm). The rectangle shows the area relating to the microscope field of view during the in-situ tensile test. Tension was applied in the X direction.

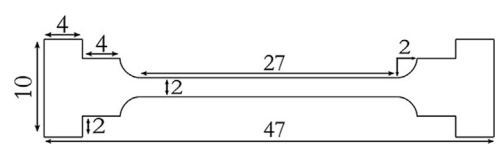

Fig. 2. Schematic of the sample adopted for the miniature tensile stage. The dimensions are in mm with a tolerance of ± 0.1 mm.

Table 2
Tensile properties of the cast material obtained from the in-situ tensile test.

Elastic modulus (GPa)	Yield strength (0.2% offset) (MPa)	Ultimate tensile strength (UTS) (MPa)	Elongation to fracture (%)
160 ± 3	280 ± 14	512 ± 12	10 ± 1

Table 1
Chemical composition of the cast material.

Element	C	Si	Mg	Cu	Mn	P	S	C_{eq}	Fe
Weight percent (wt%)	3.510	2.360	0.037	0.294	0.408	0.009	0.004	4.11	Balanced

Download English Version:

https://daneshyari.com/en/article/5455838

Download Persian Version:

https://daneshyari.com/article/5455838

Daneshyari.com